BOUNDARY PLASMA CONTROL WITH THE ERGODIC DIVERTOR

Ph. GHENDRIH, M. BECOULET, P. BEYER*
X. GARBET, A. GROSMAN, S. FERON, F. LAUGIER,
J. GUNN, B. MESLIN, P. MONIER-GARBET, C. GRISOLIA, T. LOARER, R. GUIRLET,
Association Euratom-CEA, DRFC,
CEA Cadarache,
13108 St Paul lez Durance,
France

Abstract

Ergodic divertor experiments on Tore Supra provide evidence of significant control of plasma-wall interaction [1]. Theoretical investigation of the laminar region (i.e. governed by parallel transport [2]) indicates that control of the plasma state at the target plate can be achieved with plasma states similar to that observed with the axisymmetric divertor. Analysis of the temperature field with a 2-D test particle code allows one to recover the observed spatial modulation and shows that an intrinsic barrier appears to develop at the separatrix. Energy deposition peaking, analysed with a 3-D code, is strongly reduced when moderate transverse transport is considered. Possible control of upstream parameters can thus be achieved in the ergodic region, for instance a lowering of the parallel energy flux by cross field transport.

1. INTRODUCTION

The axisymmetric divertor programme associated with the ITER project is facing conflicting physics issues. On the one hand, it must comply with the heat exhaust capability provided by the available technology. This has led to an extensive analysis of radiating plasmas in this configuration. On the other hand, high confinement is required to reach ignition. A programme focused on similar constraints is investigated experimentally on Tore Supra with the ergodic divertor [3]. The present paper is devoted to the theoretical investigation of the ergodic divertor operation. Let us first recall the main characteristics of the ergodic divertor. While the axisymmetric divertor is achieved with a toroidal current which balances the plasma current to generate an X-point, the ergodic divertor is based on the use of several helical magnetic perturbations with resonances located in the boundary plasma, typically $\rho \geq 0.8$ [3]. These modes are generated by multipolar windings. Consequences are a low perturbation current and a strong radial decay of the perturbation. On Tore Supra 6 identical in-vessel octopolar coils are located on the low field side of the torus. In standard operation, the main modes of the spectrum are $n = 6$ toroidally and $12 \leq m \leq 24$ poloidally, maximum at $m = 18$. Above a given magnitude in the perturbation current, non-linear interaction between these resonances lead to a destruction of the closed magnetic surfaces. It is convenient to estimate the stochasticity level with the Chirikov parameter σ_{Chir} [3], namely the ratio of the resonant island width to the distance between neighbouring resonances. Non-linear interaction and thus stochasticity will occur for $\sigma_{Chir} \geq 1$. The boundary safety factor, such that the Chirikov parameter is maximum at the radial location of the front face of the coils factor, characterises the ergodic divertor resonance in terms of stochasticity level, Fig. 1. The separatrix is defined as the last closed magnetic surface, hence where $\sigma_{Chir} \sim 1$ in the framework of the present definition. The optimum configuration is then found for a boundary safety factor of the order 3. On Tore Supra the current bars of the in-vessel coils are tilted with respect to the toroidal direction in order to increase the magnetic channelling of energy and particles to dedicated high heat flux target plates. One finds that the best configuration for target plate wetting is achieved for a boundary safety factor slightly smaller than 3. Using these 2 criteria to define the optimum magnetic equilibrium, one finds that the stochastic region then extends from the boundary at $q \sim 3 \pm 0.5$ to the very vicinity of the $q = 2$ surface, see Fig. 1. As a consequence, some 35 % of the plasma volume is controlled by the ergodic divertor. This volume is poloidaly and toroidaly symmetric.

---

* present address : Equipe Turbulence Plasma, LPIIM, Centre Universitaire de Saint-Jérôme, Marseille, France

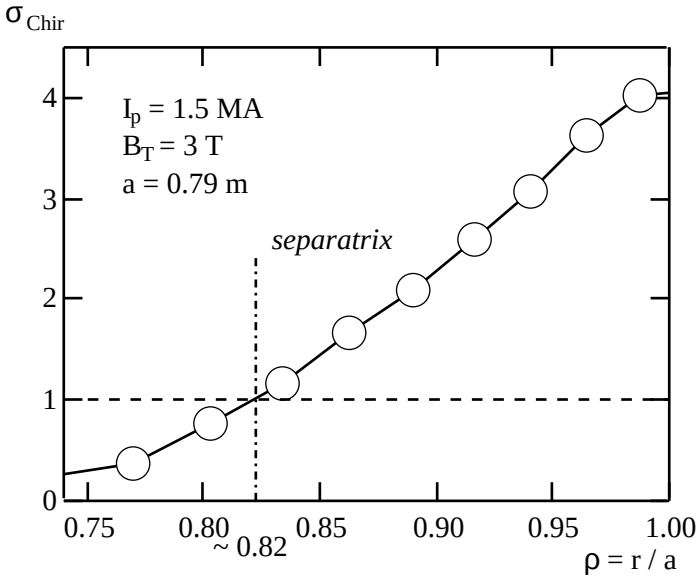

FIG. 1. Radial profile of the Chirikov parameter against ρ. In this configuration the radial extent of the stochastic boundary is 18 % of the minor radius.

However, the major recycling areas and the target plates are localised on the divertor coils on the low field of the torus. Radially, there is a significant variation from the outer radius, with large Chirikov parameter but short connection lengths to the wall, to the separatrix with the abrupt change from the stochastic region to the non stochastic region. Analysis of stochastic field lines indicates that exponential separation of neighbouring field lines characterise transport on parallel scales smaller than the Kolmogorov scale L_K, $L_K \sim 2L_{//} = 2\pi qR$, while diffusion governs field line behaviour on the longer parallel scales. Properties of a given point in the divertor volume will thus depend on the relative values of Kolmogorov scale and connection lengths, either towards the wall L_{wall} or towards the separatrix. 1-D transport in the laminar regime and control of the divertor plasma state is presented in Section 2. Test particle calculation of the temperature field with a 2-D mapping are reported in Section 3. Finally, Section 4 is devoted to the analysis of energy deposition peaking using the 3-D Mastoc field line tracing code.

2 PLASMA STATE IN REGIMES GOVERNED BY PARALLEL TRANSPORT

Analysis of plasma states with 1-D models underlines the common physics of both the axisymmetric and ergodic divertors. The specific geometrical effects are mainly probed by the neutral distribution which ignores the geometry of the magnetic field. Difference in geometry will thus translate into a difference in neutral density and location of plasma-neutral interaction. Another difference is the relationship between boundary plasma parameters and those parameters used to control the core plasma. In particular between the boundary density and the line averaged density which is a standard control parameter of discharges.

A 1-D model of the plasma state in the vicinity of the target plates is of interest insofar as parallel transport is the dominant transport channel, transverse transport remaining small. This introduces a restriction on the parallel extent which can be considered. Using a simple balance criterion, one finds the parallel coherence scale $L_\delta \sim (\chi_{//} / \chi)^{1/2} \delta$, where $\chi_{//}$ and χ are respectively the parallel and transverse heat conductivity and where δ is the transverse scale considered to bound the coherence of a given set of flux tubes. In the axisymmetric divertor, the strike point at $\delta \sim \lambda_q$ from the magnetic separatrix (λ_q is the energy flux e-folding length), then appears as the footprint of those field lines governed by parallel transport from midplane to target plate. Parallel transport in a 1-D framework will then relate midplane plasma parameters to the target plate plasma state. A more complex situation is found with the ergodic divertor since the radial extent of the stochastic boundary, from the separatrix to the target plates is typically one order of magnitude larger than λ_q. In practise, the parallel extent of the field line in 1-D model of the ergodic divertor is bounded by L_K, and δ is comparable to an unperturbed island width. This parallel extent defines the laminar region of transport [3]. Steady plasma state is investigated with particle, momentum and energy balance equations for a single fluid plasma. The classical

collisional transport heat diffusivity, $\kappa_{//} = \kappa T^{5/2}$ is used to relate the thermal flux q and the parallel temperature gradient, $q = -\kappa_{//} \nabla_{//} T$. Among the 4 required boundary conditions, 3 are standard, namely the upstream energy flux Q_{up}, the Bohm conditions at the target plate for both parallel particle flux $\Gamma_{div} = nc_s M$ with M = 1, and parallel energy flux, $Q_{div} = \gamma \Gamma_{div} T_{div}$ with $\gamma \sim 6$. M and c_s are respectively the Mach number and sound velocity. The last boundary condition, generally a particle control parameter, is related to the means used to control the plasma. In a standard fashion the gas injection is used to feed-back control specific parameters [4], for instance the line averaged density. Two critical temperatures describe the plasma state, T_Δ characterises the ionisation temperature threshold, $T_\Delta \sim 10$ eV, and $T_{//}$ characterises transport at constant energy flux with no convection :

$$T_{//} = \left[\left(Q_{up} L_{//} \right) \Big/ \left(\frac{2}{7} \kappa \right) \right]^{2/7} \qquad (1)$$

For standard ohmic shots on Tore Supra one finds $T_{//} \sim 40$ eV. The plasma temperature T_{div} at the target plate which is determined by a the combination of energy losses (Q_{div}) and particle flux build-up (Γ_{div}) will characterize the plasma state. Detachment corresponds to $T_{div} \le T_\Delta$ [5,6] while $T_\Delta \ge T_{//}$ will lead to the so-called linear regime [7]. This regime is achieved at near constant energy flux, when interaction with the neutral population is weak, hence plasma pressure is constant and convective energy flux weak over most of the field line length. The transition from linear to high recycling regimes will occur when T_{div} drops below $T_{//}$. For most light impurities, this transition also leads to radiative losses along the field line. Impurity line radiation will determined here by a given impurity concentration c_z and the radiation rate L_z (t). Let us assume that plasma pressure remains constant in this regime, $\Pi = 2n_{up} T_{up} = 2n_{div} T_{div} (1 + M_{div}^2)$, and that the energy flux is mainly conductive. The temperature profile is then determined by :

$$T_{//}^{7/2} = \frac{7}{2} \int_{T_{div}}^{T_{up}} \frac{T^{5/2} dT}{\left(1 - c_z \Pi^2 W(T) / 2 Q_{up}^2 \right)^{1/2}} \quad ; \quad W(T) = \int_T^{T_{up}} \frac{\kappa_{//} L_z(T) dT}{T^2} \qquad (2)$$

In the attached regime the pressure is related to the energy and particle flux at the sheath boundary so that the plasma pressure is defined by Q_{up}, the upstream energy flux and given T_{div}.

$$\frac{\Pi}{Q_{up}} = \left[\frac{\gamma^2 M_{div}^2}{2 \left(1 + M_{div}^2 \right)^2} \frac{T_{div}}{m_i} + \frac{c_z}{2} W(T_{div}) \right]^{-1/2} \qquad (3)$$

While the plasma pressure in the linear regime is only determined by the sheath boundary conditions, one observes a significant drop when radiation becomes significant. One can determine a critical impurity concentration such that radiation rather than boundary conditions govern the plasma pressure, typically a few percent of oxygen at $T_{div} \sim 30$ eV. This drop in pressure in the attached case is not however a parallel drop along the field lines as would characterise detachment.

The complete calculation from a given T_{div} to the corresponding value of n_{up} for a given upstream energy flux and given impurity concentration indicates that the decrease in pressure due to radiation does not lead to a decrease of the divertor plasma density. Rather in the high recycling regime, peaked radiation rates yield bifurcation points such that a given n_{up} allows for three possible values of n_{div}, one branch being unstable, Fig. 2. As a result one observes a much stronger increase of the divertor plasma density than expected from the cubic dependence which holds with no radiation [7]. The hysteresis induced by radiation is strongly linked to the peaking of the radiation rate [8]. Furthermore, the temperature reached beyond the bifurcation point also depends on the radiation rate. In the case shown for an oxygen like radiation, one finds that the low temperature stable branch is reached around 8 eV. For carbon (or deuterium) in near coronal conditions, the bifurcation will lead to a lower temperature in the 5 eV range.

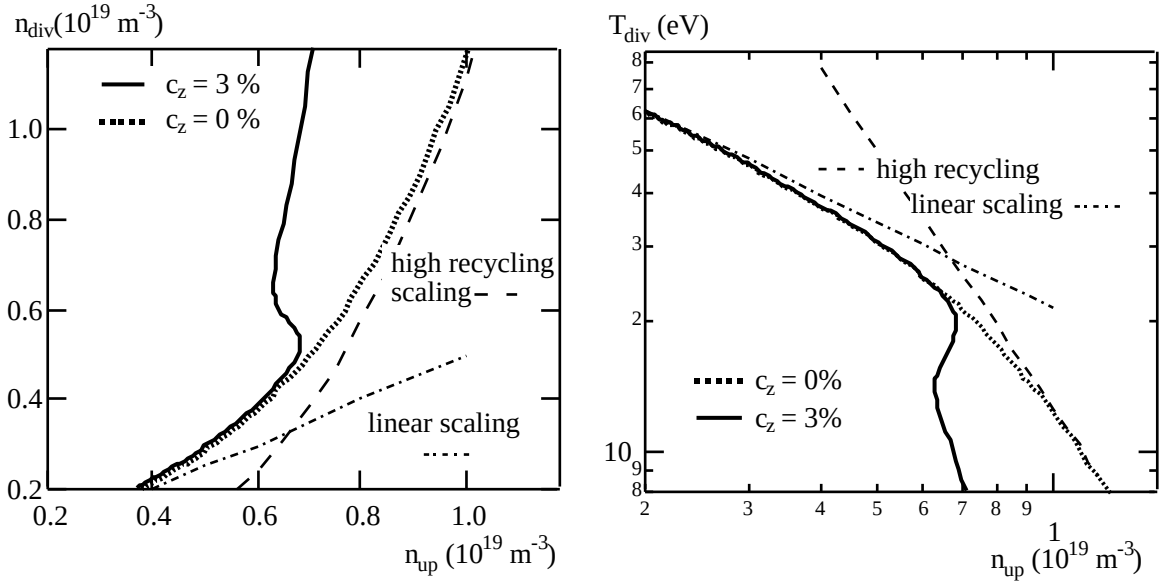

FIG. 2. Bifurcation in the high recycling regime, density regimes (left) in linear scale and temperature regimes (right), logarithmic scale.

Comparing these results to the experiments indicates that the level of carbon and oxygen impurity can decrease very significantly as the core and divertor density rise. This will tend to smooth out the bifurcation aspect. Furthermore, density ramps are usually used experimentally. The sequence of divertor states can then correspond to transients states which can depart significantly from the steady state regimes, especially near the bifurcation points. As density is increased, coupling of the temperature field to the density field becomes more important, especially as soon as momentum loss plays a role. Coupling to the Bohm boundary constraint on the Mach number and the Mach number profile is then important [9]. In order to analyse the Mach number profile along the magnetic field (curvilinear abscissa s), let us introduce $\mathcal{M} = (2|M|) / (1 + M^2)$ such that :

$$\mathcal{M} = \frac{4T|\Gamma|}{\Pi c_s} \quad ; \quad \frac{d\mathcal{M}}{\mathcal{M}\ ds} = \frac{1}{2}\left[\frac{1}{T}\frac{dT}{ds} - \left(\frac{\mathcal{M}}{L_{cx}} + \frac{2}{|M|\ L_I}\right)\right] \qquad (4)$$

The scales L_{CX} , L_I are the charge exchange and ionisation mean free path $L_{CX} = c_S / (n_N \langle\sigma v\rangle_{cx})$, $L_I = c_S / (n_N \langle\sigma v\rangle_I)$. Two sets of terms govern the parallel variation of the Mach number, the positive temperature gradient induces a reduction of the Mach number as one approaches the target plates. Conversely, the parallel pressure drop towards the target plate and the particle flux increase to the target plate generate the standard increase of the Mach number towards the target plate. Strong temperature gradients thus allow for a non-monotonic behaviour of $\mathcal{M}$ and thus of the Mach number. It is to be noted that this extremum in the Mach number also allows for a transition to detachment of the Mach = 1 front. Using Eq. (4), one can define an upper limit of the temperature at the Mach number extremum which depends on the parallel heat flux q and neutral density n_N.

$$\frac{T}{10\ eV} \le \left[\frac{3.12510^{-3}\ |q|}{n_N \langle\sigma v\rangle_{cx}}\right] \Big/ \left[\mathcal{M} + \frac{2\langle\sigma v\rangle_I}{|M|\ \langle\sigma v\rangle_{cx}}\right]^{1/3} \qquad (5)$$

In a regime with a significant heat flux q ~ 10 MW m^{-2} and moderate neutral density $n_N \sim 10^{18}\ m^{-3}$, one can observe a decrease of the Mach number for a relatively high plasma temperature of order 10 eV. The existence of an extremum of the Mach number upstream of the target plate is then only possible if the available heat flux decreases to zero, allowing for a weak temperature gradient. The Mach number extremum is thus located in the vicinity of the transition from conductive to convective energy flow, Fig. 3.

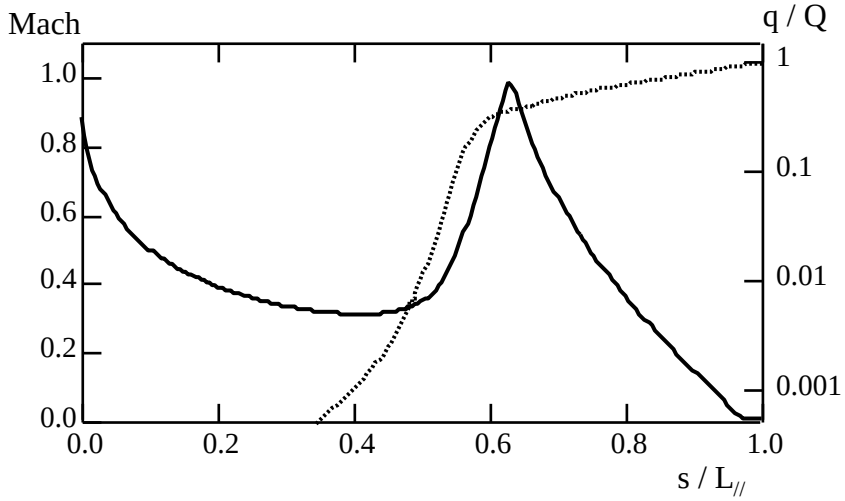

FIG. 3. Profiles of the Mach number and of the ratio of the conducted energy flux q over the total energy flux Q against the curvilinear abscissa s normalised to the field line length $L_{//}$.

Since detachment is readily associated to the transition from conducted to convective energy flow, it is possible to use the Mach number extremum to monitor the location of the detachment front [9]. The 1-D modelling thus provides a qualitative frame of understanding for the radiative divertor experiments. Departure from standard observations in the axisymmetric divertor configuration can be related to geometrical differences in neutral recirculation -with a more symmetric and low density neutral population- as well as to the impact of the ergodic region on the energy flux.

3 TEMPERATURE MODULATIONS AND SEPARATRIX TRANSPORT BARRIER

Transport in the ergodic divertor volume can be modelled by a succession of steps where parallel transport dominates. The transition from a given parallel step to the following step is governed by transverse transport. In order to investigate the structure of the temperature field beyond the parallel scale L_K, one has to consider the 3-D structure of the field lines. Of particular importance are the combination of parallel and transverse steps which minimise the distance (as measured by heat diffusion) from the source, say the separatrix, to the sinks, mainly the target plates in-between the current bars of the divertor coils [10]. To tackle this issue, particle test transport has been considered. The 3-D parallel motion of energy is simplified to a mapping. Indeed, the small toroidal extent of the Tore Supra divertor coils allows one to generate a 2-D mapping which follows the trajectory of the field lines in the poloidal plane. Cross field transport, modelled by a random step of given magnitude, is superimposed to parallel transport. The test particle source is located within the closed magnetic surfaces, while the perfectly absorbing wall is the sink at $\rho = 1$. Magnitude of cross field transport particle parallel velocity are constant throughout the divertor volume. Integration of the physics discussed in Section 2 is too demanding to be addressed with the rather simple codes presently available. Unfolding the density of test particles in terms of a temperature field would require to consistently compute the particle density map. Furthermore, some kind of iteration procedure would be needed to adapt the ratio between parallel and transverse transport to the computed temperature field. However, one can expect many features of the test particle distribution to be representative of the temperature field. This straightforward modelling of the energy transport in the divertor volume has allowed one to tackle two issues. First, the radial and poloidal temperature modulations observed in the experiments have been recovered [10]. One can show that the temperature maxima are located at the radial and poloidal positions characterised by parallel connection properties to the test particle source [1]. As a consequence, the 2-D structure of the test particle density is close to that of the connection lengths in a poloidal section. One can show that the magnitude of the modulations of the test particle density increases as one decreases the noise level, i.e. transverse transport [10]. More interestingly, in the vicinity of the separatrix, one finds an increase of the test particle density gradient so the test particle density profile recovers the profile one would expect in a limiter configuration, Fig. 4. This is observed when the transverse diffusion coefficient is smaller than the effective transverse diffusion due to field line stochasticity with $\sigma_{Chir} \sim 1$.

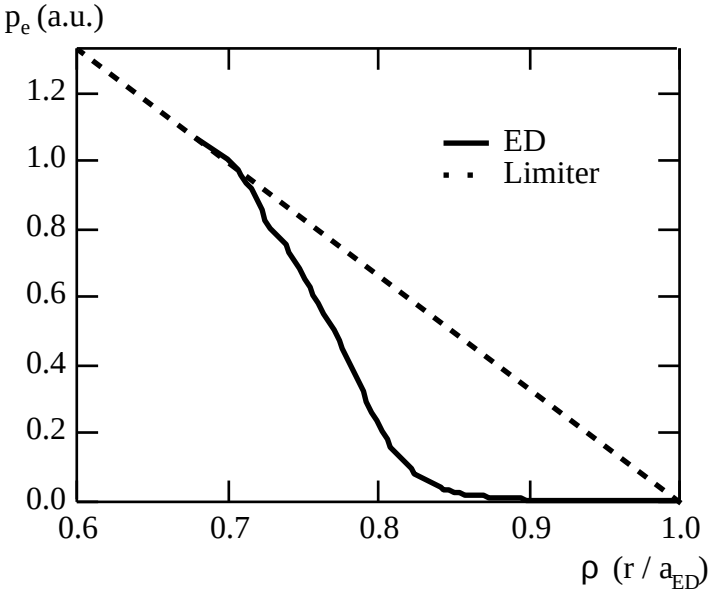

FIG. 4. Test particle profile : towards the core ρ ~ 0.7, standard gradient (extending to ρ = 1 in the limiter configuration), boundary ρ ~ 1, flat and low density due to a strong deconfinement, intermediate region, ρ ~ 0.8, increase of the density gradient.

It appears to extend in the region with $\sigma_{Chir} \leq 1$ [10]. Although one can relate such a behaviour to trapping mechanism in remnant island structures in a region of strongly varying transport properties, further investigation is required to determine the proper driving mechanism. It is to be noted that a similar behaviour has been observed in a Fermi map slightly modified in order to properly represent the radial Chirikov profile in the vicinity of the divertor separatrix.

Along with this rough simulation of energy transport in the divertor volume, 3-D codes have been developed. With a reduced number of poloidal modes, one has investigated the effect of stochasticity on ballooning modes. This has shown that the ballooning modes coupled to the perturbation (toroidal mode numbers multiple of 6) are characterised by a reduced level of pressure fluctuations while the overall transport is not reduced due to the increase in the electric potential gradients [11]. These results are in good qualitative agreement with experimental observation of a reduced density fluctuations [12], especially at small k , while transverse transport appears to remain large. Another 3-D code with given cross field transport but large poloidal and toroidal spectrum is being used to analyse the temperature field. First results indicate that one recover the temperature modulations provided one fully accounts for all the non-linear features and especially of the strong temperature dependence of parallel transport. It also appears that non linear coupling between modes of small amplitude in the divertor spectrum and strong temperature gradients can generate significant contributions. These calculations as well as the modelling effort with the test particles demonstrate that the effective diffusion coefficients [13] do not allow one to capture the complexity of the temperature field in a stochastic boundary. One can verify that the mean temperature gradient, with a radial averaging over several resonances, is in agreement with effective diffusion coefficients [13]. These studies cannot determine the properties on the scale of the stochastic random step nor the effects related to the finite extent of the stochastic boundary.

4 ENERGY DEPOSITION

Peaking of the energy flux onto the target plates is of particular importance for a safe operation of the divertor in steady state conditions. As one can expect from the 3-D properties of the temperature field, energy deposition must also be investigated on the basis of a 3-D calculation. The close relationship between the pattern of energy deposition and the connection properties of field lines over one poloidal rotation has led us to derive the energy flux deposition capability of a given field line from its geometrical properties. Let consider a set of field lines which act as a distribution of sinks in volume at various radial locations and characterized by

various efficiencies depending on the parallel connexion length to the wall. In a 1D approximation the energy balance equation is simplified to :

$$\frac{dQ}{dr} = P_{loss}(r) \quad ; \quad P_{loss}(r) \approx -\frac{Q_{//}}{L_{eff}(r)} \qquad (6)$$

The parallel scale $L_{eff}(r)$ which is now introduced describes the efficiency of the sinks located at r and which transfer an energy flux $Q_{//} \sim - n \chi_{//} T / L_{eff}$. In a slab geometry and after introducing the transverse heat diffusivity $n \chi$ ones obtains a diffusion equation with a radially varying sink term $\chi_{//} /(\chi L_{eff}^{2})$. In order to account for the exponential amplification of transverse transport due to stochasticity which is not included in the left hand of Eq. (6), one must consider $L_{eff}(r) = L_{wall}(r) \exp(L_{wall}(r) / L_{//})$. Due to the exponentially increasing probability of the energy to be transferred to a neighbouring flux line via transverse transport, the effective connexion length appears to increase exponentially as the connexion length increases. Using a WKB procedure as in Ref. [2], one can computes the parallel loss channel of transverse energy flux Q_{wall}.

$$Q_{wall}(r) \quad \frac{1}{\sqrt{L_{eff}(r)}} \exp\left(-\int_0^r \sqrt{\frac{\chi_{//}}{\chi}} \frac{dr}{L_{eff}(r)}\right) \qquad (7)$$

The non monotonic behaviour of this loss function is a balance between the increasing efficiency of the parallel loss channel to the wall as the radius increases ($\lambda_q(r) = \sqrt{(\chi / \chi_{//})}\, L_{eff}(r)$ contribution) and the exponential decrease of the available transverse energy flux. The transport balance which governs Q_{wall} defines the radially varying radial scale of energy deposition, $\lambda_q(r) = \sqrt{(\chi / \chi_{//})}\, L_{eff}(r)$. The maximum of Q_{wall} then occurs at $\bar{\lambda}_q = \sqrt{(\chi / \chi_{//})}\, L_{eff}(a - \bar{\lambda}_q)$. The calculation of the transverse energy flux leaking to the wall via transverse transport, Q_{wall}, enables one to compute in principle the profile of the transverse energy flux using a reference radius r_0 near the separatrix of the stochastic boundary, $Q(r) = r_0 Q(r_0) / r - Q_{wall}(r)$. The energy extraction capability of a given field line is then characterised by the minimum radius r_{min} reached over the finite parallel excursion of $L_{//}$. In this framework, the parallel energy flux for a given field line $Q_{//}$ is thus proportional to $Q(r_{min})$. For a set of field lines initiated along a midplane target plate, one can then compute the radial penetration r_{min} with the Mastoc code.

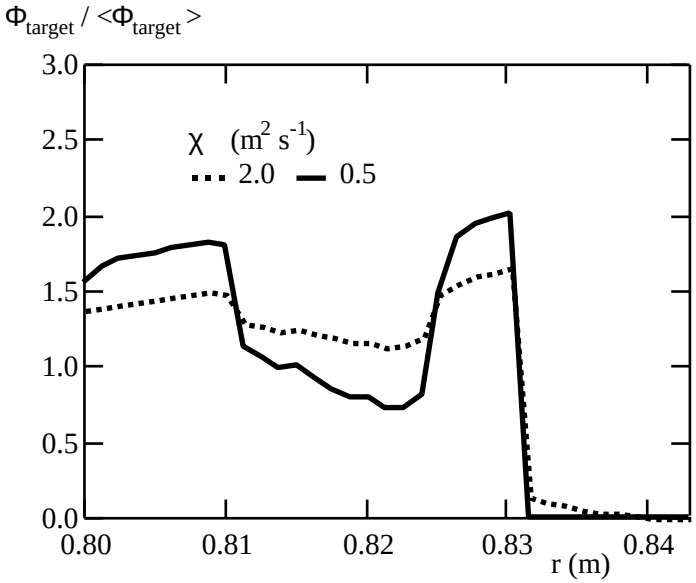

FIG. 6. Peaking factor of the energy flux to the target plate versus the radius of the impinging point on the target plate.

A significant change in the heat deposition is then observed (as expected) when transverse transport is changed. At given available total energy flux characterized by <Q >, the increase of χ leads to a lowering of the available energy flux for field lines which exhibit a large penetration and an increase of the available energy flux to the field lines with a small radial penetration. The chosen procedure only provides a means to compute the peaking factor of energy deposition, the average energy flux remaining to be determined. In a final step, the calculation of the impinging angle of the field lines onto the target plate, θ_{imp}, allows one to calculate the relevant energy flux Φ_{target}, Fig. 6. In this plot, the peaking factor $\Phi_{target} / <\Phi_{target}>$ is nearly flat over all the wetted area as soon as $\chi \sim 2$ m s^{-2}. At this level of cross field transport, the energy flux thus appears to be totally redistributed on all the flux tubes impinging onto the target plates. Experimentally, the reduction in the peaking factor is observed with core plasma heating [2]. Accordingly, the control parameter Q_{up}, namely the upstream energy flux, in the 1-D model of Section 2 will exhibit a reduced dependence on the injected power than would be expected.

5 CONCLUSION

The theoretical analysis of transport in a stochastic boundary is shown to exhibit the physics of the standard axisymmetric divertor on connection lengths of the order of one poloidal rotation. This provides a powerful tool to interpret the observed states of the plasma at the divertor target plate. The relationship between the upstream parameters and the control parameters of the core plasma require a comprehensive analysis of the transport throughout the divertor volume. Regarding, energy deposition, stochasticity and its mixing properties, provides a statistical basis to compute the energy extraction capability of a given field line. This analysis allows one to translate the geometrical feature of the field line, and in particular its radial penetration, into an energy extraction capability at given transverse transport. For specific field lines, the exact geometry of the field lines computed with the 3-D field line tracing code Mastoc is then sufficient to calculate the peaking factor of the energy flux at the impinging point onto the target plate. This calculation shows that cross field transport tends to rapidly smooth out the deposition peaking reported for the low density ohmic shots. Investigation with 2-D test particle calculation or with full 3-D codes is being used to determine the temperature field. Both method allow us to recover the temperature modulations and again so associate them to low cross field transport. In a similar regime, the density of test particles is shown to exhibit a marked increase in gradient in the vicinity of the separatrix. This increase is sufficient to balance the loss in confinement in the very outer divertor volume where parallel transport strongly deconfines energy. Theoretical analysis of the ergodic divertor physics now permits a qualitative understanding of the experiments. However, an integration effort of the various achievements is still required to assess and quantify the results.

References

[1]Tore Supra team presented by Ph. Ghendrih, Plasma Phys. Contr. Fusion, **39** (1997) B207.
[2]A. Grosman et al., Contributions to Plasma Physics, **??**.
[3]Ph. Ghendrih, A. Grosman and H. Capes, Plasma Phys. Contr. Fus. **38** (1996) 1653.
[4]C. Grisolia et al., "Feedback control of high radiative plasmas in Tore Supra" to be published in J. Nucl. Mater.
[5]Ph. Ghendrih, Phys. Plasmas **1** (1994) 1929.
[6]A. Loarte, Nucl. Fusion **38** (1998) 331.
[7]C. S. Pitcher and P.C. Stangeby, Plasma Phys. Contr. Fus., **39**(1997)779.
[8]H. Capes, Ph. Ghendrih and A. Samain, Phys. Fluids, **B4**(1992)1287.
[9]Ph. Ghendrih et al., "Comparison of Ergodic and Axisymmetric Divertors" to be published in J. Nucl. Mater.
[10]S. Féron, PhD Thesis "Transport de la chaleur dans un champ magnétique chaotique," Report EUR-CEA-FC-1616, December 1997.
[11]P; Beyer et al., "2D and 3D boundary turbulence studies" to be published in Plasma Phys. Contr. Fus.
[12]J. Payan, X. Garbet, J.-H. Chatenet et al., Nucl. Fus., **35**(1995)1357.
[13]Ph. Ghendrih et al., in *Transport, Chaos and Plasma Physics 2*, Editors S. Benkadda, F. Doveil and Y. Elskens, World Scientific, Singapore 1996, p. 179.